Date: 2025/11/17

論文情報

アクセス権	open access
タイトル	Flexible Optical Tactile Force Sensor to Conduct Measurements From the Back of the Hand
著者	Kosuke Ando Minon Kushihashi Hiroshi Kawaguchi Shintaro Izumi
言語	English
収録物名	IEEE Sensors Journal
巻（号）	25(8)
ページ	12872-12880
出版社	Institute of Electrical and Electronics Engineers (IEEE)
刊行日	2025/04/15
公開日	2025/04/30
権利	
DOI	https://doi.org/10.1109/JSEN.2025.3545137
備考	一部の著者については、顔写真掲載の承諾が得られなかったため黒塗りで記載をしています。

Flexible Optical Tactile Force Sensor to Conduct Measurements From the Back of the Hand

Kosuke Ando, Minon Kushihashi, *Graduate Student Member, IEEE*, Hiroshi Kawaguchi, *Member, IEEE*, and Shintaro Izumi, *Member, IEEE*

***Abstract* —The accurate and nonintrusive measurement of tactile information from the hand is crucial for various applications, such as in healthcare, robotics, augmented reality (AR)/virtual reality (VR), and sports. However, current technologies often hinder tactile sensation or restrict measurements to specific areas of the hands. This study presents a novel flexible optical tactile force sensor that can be attached to the back of the hand, thereby enabling the comprehensive measurement of tactile information without compromising natural tactile perception. This sensor enables the simultaneous estimation of pressure, force direction, and pulse wave information, thereby merging biomechanical and physiological monitoring. We demonstrated the sensor's capability to estimate both the pressure and direction of the applied force by affixing the flexible optical sensor to the back of the hand, comparable with conventional palm-side sensors while preserving tactile sensation. This sensor simultaneously measures skin deformation and changes in blood volume, enabling the real-time acquisition of force and pulse wave data. Our innovative approach enables accurate and nonintrusive measurement of the tactile force on the hand and fingers while providing valuable physiological insights through pulse wave analysis. These advancements hold significant promise for healthcare applications, where the real-time monitoring of mechanical and cardiovascular data could significantly enhance diagnostic capabilities.**

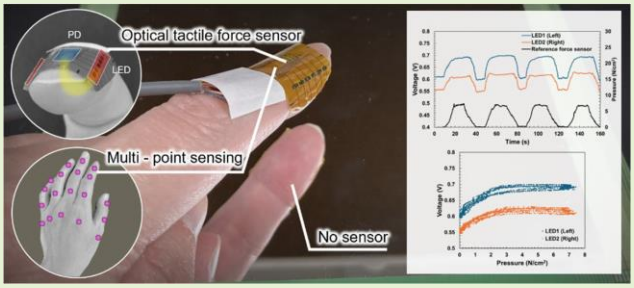

***Index Terms*— Force sensor, haptics, optical sensor, tactile.**

I. Introduction

DEVICES designed to measure human tactile information are anticipated to be utilized in various applications across various industries, including healthcare, robotics, entertainment, augmented reality (AR)/virtual reality (VR), and sports [1], [2], [3]. The hand, in particular, has numerous tactile receptors, making it a focal point for ongoing research into tactile measurement devices.

Tactile perception refers to the ability to sense stimuli through sensory receptors located on and within the skin's surface, enabling individuals to perceive the texture, temperature, and vibrations of objects [4], [5]. Previous studies on tactile sensing have primarily focused on measuring the deformation of fingers caused by tactile forces to determine pressure and force direction [6], [7], [8], [9], [10]. Simple implementations involve placing sensors between objects and fingers, such as glove-type sensor devices or flexible adhesive sensors. However, these methods often hinder natural tactile sensation.

Consequently, measurement methods that do not interfere with touch are highly required, resulting in the development of methods that can be affixed to the sides or fingernails. For example, approaches that utilize piezoelectric films or strain sensors on the sides of fingers to measure deformation have been proposed [11]. Additionally, techniques that measure deformation or color changes in fingernails have been developed to estimate the pressure and force direction without interfering with touch [12], [13], [14]. Various sensing methods have been explored, including piezoelectric, strain-based, ultrasonic, micro-electro-mechanical systems (MEMSs), and optical sensors [15], [16]. In optical methods, the direction of pressure and force can be inferred by observing color changes within the nail when pressure is applied [17], [18]. However, these nonobstructive methods for measuring tactile information are limited to the nails or fingertips, making it challenging to capture tactile information from the

Received 10 December 2024; revised 14 February 2025; accepted 19 February 2025. Date of publication 3 March 2025; date of current version 16 April 2025. This work was supported in part by Japan Science and Technology Agency (JST) under Grant JPMJPF2115 and in part by the KOSÉ Cosmetology Research Foundation. The associate editor coordinating the review of this article and approving it for publication was Dr. Juan A. Lenero-Bardallo. *(Corresponding author: Shintaro Izumi.)*

This work involved human subjects or animals in its research. Approval of all ethical and experimental procedures and protocols was granted by the Ethics Committee of Kobe University under Application No. 2024–3, and performed in line with the Declaration of Helsinki.

Kosuke Ando is with the Graduate School of Science, Technology and Innovation, Kobe University, Kobe 657-8501, Japan, and also with the Technology Development Headquarters, KONICA MINOLTA Inc., Tokyo 192-8505, Japan.

Minon Kushihashi, Hiroshi Kawaguchi, and Shintaro Izumi are with the Graduate School of Science, Technology and Innovation, Kobe University, Kobe 657-8501, Japan (e-mail: shin@cs28.cs.kobe-u.ac.jp).

Digital Object Identifier 10.1109/JSEN.2025.3545137

TABLE I
COMPARISON WITH RELATED WORKS

[Ref.]	[Sensor]	[Principle] Skin surface deformation	[Principle] Internal tissue deformation	[Principle] Blood volume change	[Sensor adaptability] Preserves natural tactile perception	[Sensor adaptability] Works beyond fingertips
–	**LEDs and photodiode**	**Yes**	**Yes**	**Yes**	**Yes**	**Yes**
[1]	Piezoresistive force sensor	No	No	No	No	Yes
[10]	LEDs and cameras	No	No	No	Yes	No
[11]	Strain gauges and accelerometer	Yes	No	No	Yes	No
[12]	LEDs and photodiodes	No	No	Yes	Yes	No
[19]	LEDs and photodiodes	Yes	No	No	Yes	No

entire hand without interfering with the sense of touch [19]. Furthermore, the measurement of finger deformation from the body surface limits the precision of these methods.

To address these challenges, we developed a cutting-edge flexible optical tactile force sensor that can be seamlessly attached to the back of the hand and fingers, surpassing the constraints of conventional tactile sensors. In the proposed method, infrared light-emitting diodes (LEDs) and photodiodes (PDs) are utilized on a flexible substrate that adheres seamlessly to the back of the hand or fingers. LEDs and PDs are constructed using inorganic materials, with a flexible printed circuit (FPC) serving as the substrate, allowing conformity with the skin. Most of the contact area with the skin comprises the FPC, thereby minimizing the impact of the rigidity of the PDs and LEDs. However, if the device is not securely attached, part of the LED emission may reflect off the skin surface, decreasing the amount of light received by the PD. Particularly, reattachment is required to ensure accurate measurement if the LED detaches from the skin. A portion of the light emitted from the LEDs is reflected off the skin's surface, whereas the remainder penetrates the tissue. The light that scatters within the tissue and is not absorbed re-emerges and is detected by the PD. When pressure is applied to the hand or fingers, resulting in deformation, the light path is altered, along with the blood volume within the vessels. The modification in the propagation path and blood volume impacts the amount of light reflected and measured by the PD, enabling the precise measurement of tissue deformation and estimation of the applied tactile force. Moreover, we can capture tissue deformation in intricate detail and estimate not only the force's magnitude but also its direction by arranging multiple light sources in an array and utilizing time-division illumination.

Our proposed optical measurement method shares similarities with the configurations utilized in photoplethysmography (PPG) and oxygen saturation (SpO2) measurement [20], [21], [22], [23], [24], [25], [26]. Although finger deformation is a major source of noise in PPG and SpO2 measurements, our method leverages this deformation [27], [28], [29], [30], [31], [32]. Furthermore, the performance of the proposed method can be enhanced by leveraging the extensive research conducted on the principles of PPG and SpO2 measurement, as well as strategies for accuracy enhancement, cost reduction, and noise elimination. Another key advantage of our device is its structural similarity to PPG and SpO2 sensors, enabling the simultaneous measurement of pulse waves and SpO2 alongside tactile force estimation.

This allows for the collection of data related to tissue deformation and pulse wave activity. Despite the presence of electrical noise from the power supply and environmental light in the signal, we can effectively separate these signals and noise using analog circuit filters and digital signal processing post analog-to-digital conversion. The direction of the force can be estimated by utilizing clustering techniques. A comparison of key characteristics between this study and related studies is presented in Table I.

We fabricated a prototype device (Fig. 1) based on our proposed method and evaluated its performance in measuring tactile force. The device was affixed to various areas of the back of the hand and fingers, with tactile force and direction measured by interacting with a three-axis force sensor as a reference. We evaluated the accuracy of the tactile force estimation by synchronizing the output of the reference sensor and timing data. Based on the experimental results, our sensor achieved a resolution of 0.1 N/cm^2 and dynamic range of up to 2 N/cm^2. Furthermore, the device could discriminate between the upward, downward, left, and right force directions with over 94% accuracy.

The tactile sensor developed in this study not only matches the accuracy of existing commercial tactile sensors but also offers the unique advantage of not obstructing the user's tactile sensation. Unlike previous research aimed at nonobstructive tactile sensing, our method allows for measurements over a wider area of the hand, beyond just the fingertips, while providing higher precision. Furthermore, by analyzing the pulse wave data alongside force information, our method demonstrates significant potential for broader applications in fields, such as healthcare and sports. In healthcare, our sensor holds great promise for real-time monitoring of mechanical and cardiovascular data, which can significantly enhance diagnostics. In sports, the combination of cardiovascular feedback with precise force measurement can lead to enhanced performance analysis. The proposed sensor, with a resolution of 0.1 N/cm^2 and dynamic window of 0–2 N/cm^2, has versatile applications in both the medical and sports industries.

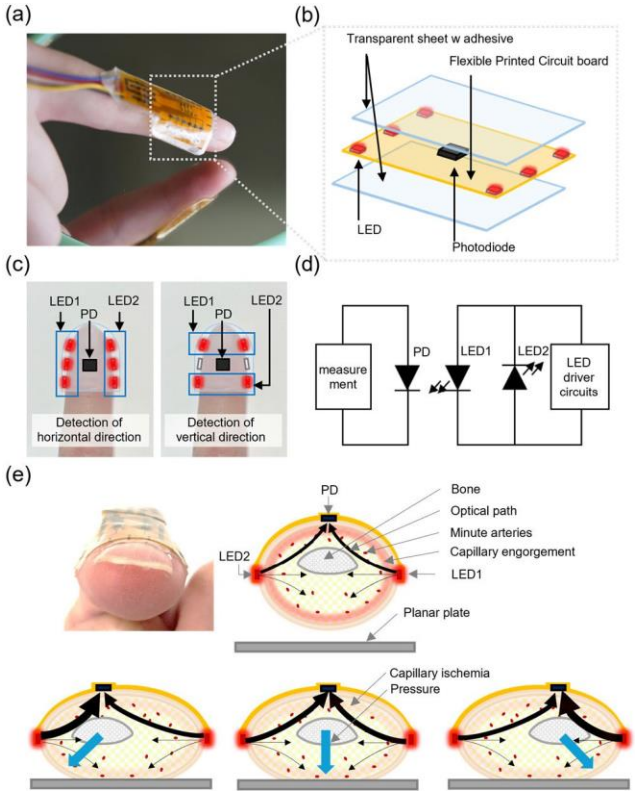

Fig. 1. Design of the flexible optical tactile force sensor. (a) Positioned on the back of the finger, no obstruction to touch. (b) PDs and LEDs protected by transparent sheet. (c) Time division detects force direction and magnitude. (d) Circuit similar to PPG sensors. (e) Optical path and detection.

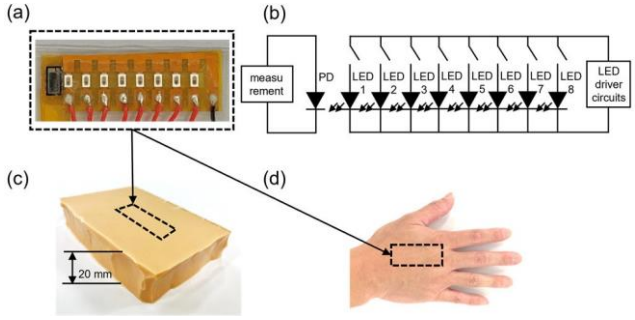

Fig. 2. Experiment for designing the distance between an LED and PD. (a) Experimental FPC with multiple LEDs at various distances from the PD, with a PD-LED distance of 1 mm and LED interval of 3 mm. (b) Circuit block diagram of the board shown in (a) and (c) attachment position on the biological tissue simulant. (d) Attachment position at the back of the hand.

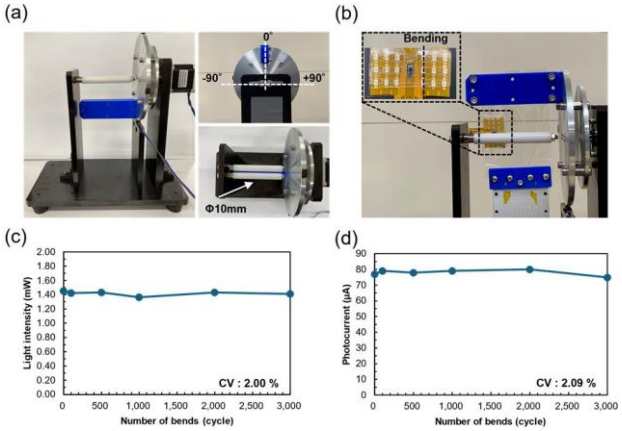

Fig. 3. Flexural durability test of the proposed sensor. (a) Photograph of the testing machine bending from 0° to ±90°. (b) Sensor attached to the testing machine. (c) LED output change during bending cycles. (d) PD light reception change during bending cycles.

Specifically, in sports, the sensor's measurement range is ideal for accurately detecting grip pressure during activities, such as golf putting (0.2–2 N/cm^2).

In conclusion, the proposed flexible optical tactile force sensor significantly enhances the performance and reliability of tactile interfaces across various applications.

II. Method

A. Implementation of the Sensor Device

The proposed sensor comprises a three-layer structure with light-emitting and light-receiving components mounted on an FPC sandwiched between two transparent urethane sheets. Multiple LEDs (VSMY5850X01, Vishay Intertechnology) were simultaneously illuminated in the light-emitting section to minimize the influence of the contact position on the skin. The light-receiving section utilizes PDs with a peak sensitivity of $\lambda_p = 850$ nm (VEMD8080CT-ND, Vishay Intertechnology) to detect the light emitted from the light-emitting section. A flexible circuit board with one light-receiving and eight light-emitting components was prototyped to determine their optimal arrangement. The distances from the light-receiving component to each light-emitting component were set at 1, 3, 6, 9, 12, 15, 18, and 21 mm. The positional relationship between the light-emitting and light-receiving components of the proposed sensor was designed based on the measurements obtained using this board (Fig. 2).

B. Evaluation of Physical Durability

The prototype flexible optical sensor was designed to bend and conform to the body, making it crucial to evaluate the sensor's flexural durability. The custom-made bending test apparatus utilized for the evaluation is shown in Fig. 3(a) and (b). During the bending test, tension was applied to the sensor using a weight. One end of the sensor (End 1) was fixed in place, whereas a weight of approximately 120 g was attached to the other end (End 2) to maintain tension in a static state. The bending section was then wrapped around a cylindrical rod with a radius of $r = 5$ mm, and End 1 was moved from an initial angle of 0°, bending from $-90°$ to $+90°$ as one cycle, for 3000 cycles. The light intensity of the emitting section and photocurrent of the receiving section were measured to determine the impact of the number of bending cycles on the sensor's performance, validating the absence of an impact. The light intensity of the emitting section was evaluated using a power meter (PM100D, Thorlabs) by measuring the photocurrent when the sensor's PD was in close contact with each LED [Fig. 3(c)]. To evaluate the stability of the emitted light intensity under bending tests, the coefficient of variation (CV) was calculated. The findings revealed a CV of 2.00%, indicating that the emitted light

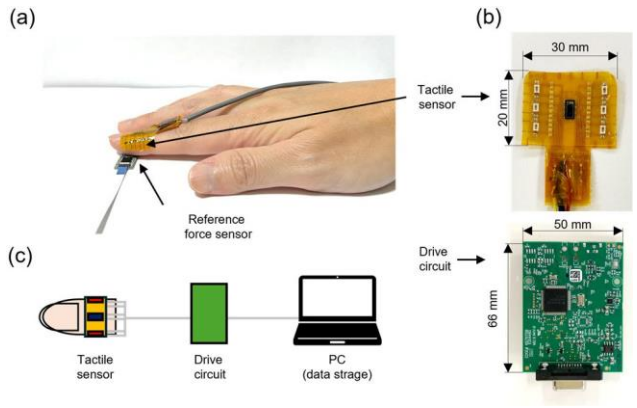

Fig. 4. Implementation of the module. (a) Module and its attachment to the back of the hand. (b) Components of the module. (c) Communication with a PC. Real-time data reading can be performed at a sampling rate of 1 kHz.

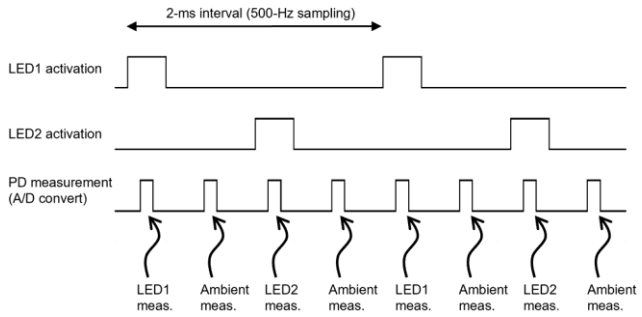

Fig. 5. LEDs were divided into two groups and were alternately illuminated, with a nonilluminated period inserted between them to measure ambient light. Interval: 2 ms.

intensity maintained high stability. The photocurrent of the receiving section was evaluated under conditions in which the LEDs of the emitting section were in close contact with the PD [Fig. 3(d)]. CV was calculated to evaluate the stability of the photocurrent in the receiving section, yielding 2.09%, validating its high stability. These results demonstrate that the optical characteristics of the sensor remain stable even after repeated bending cycles, ensuring its durability in practical applications.

C. Measurement Environment

The prototype sensor device was connected to a measurement circuit (AFE4403EVM, Texas Instruments) and linked to a Windows PC for data acquisition (Fig. 4). Parameter control and data acquisition were performed using a dedicated application (SLAC672, Texas Instruments). The sampling frequency was set to 1 kHz, and pulsewidth modulation control was utilized to sequentially measure the signals from each light-emitting section and the nonemitting state. A current of 6 mA per element traversed each LED in the emitting section, and the PD was configured with a feedback resistor of 10 kΩ to amplify the output signal for data acquisition.

D. Signal Processing

To quantitatively evaluate the tactile force, the proposed sensor was affixed to the back of the hand, whereas a reference force sensor (6DoF-P18, Touchence) was applied to the fingertip for simultaneous measurement. To mitigate external influences, such as ambient light, the analysis focused on the disparity between the signals captured during the emitting and nonemitting states. Furthermore, these differential data were separated into pulse wave and tactile force data using a moving average process. The pressure and force directions were estimated for the tactile force data. Pressure estimation involved assessing the correlation between the outputs of the proposed and reference sensor, whereas force direction estimation involved clustering the signal intensities from each light-emitting section.

This research was conducted in compliance with the ethical standards set forth by Kobe University and the Declaration of Helsinki. Ethical approval for experiments involving human participants was granted by the Ethics Committee of Kobe University (Approval number: 2024–3).

III. Results

A. Design of the Flexible Optical Tactile Force Sensor

The structure of the flexible optical tactile force sensor is shown in Fig. 1. The sensor, fabricated from flexible materials, provides a comfortable and conforming fit to the hand, as shown in Fig. 1(a). The sensor comprises two parts: the bioadhesive and sensing sections. The sensor is designed with the bioadhesive section positioned above the sensing section, allowing direct contact with the skin on top. The bioadhesive section utilizes biocompatible adhesive and transparent urethane sheets [Fig. 1(b)]. The sensing section comprises a FPC board (FPC), LED, and light-receiving element (PD). The light-emitting components on the circuit board are strategically positioned on the sides of the fingers to detect pressure direction, whether vertical or horizontal [Fig. 1(c)]. The FPC included circuits for driving the light-emitting and light-receiving components [Fig. 1(d)]. The optical path and detection mechanism differ based on the presence or absence of applied pressure [Fig. 1(e)]. When pressure is applied, increased light scattering and absorption result in alterations in the detected signal at the PD.

To measure tactile sensation without hindering the hand's ability to feel, the sensor utilizes a method in which light is irradiated from the back of the hand and the reflected light is measured [33], [34]. The amount of light that penetrated the tissue varied with the wavelength; however, the proposed method utilized infrared light, which can penetrate deeper into the tissue [35]. The sensor's light-emitting and light-receiving components were constructed using infrared LEDs with a peak wavelength of 850 nm and silicon PDs with a peak sensitivity at 850 nm. The LED in the light-emitting section was controlled through time division to estimate the direction of the tactile force and minimize the influence of ambient light [Figs. 1(c) and 5]. For example, by rapidly alternating between three states—left-side LEDs ON, right-side LEDs ON, and light OFF—the sensor can detect differences in light absorption caused by finger deformation along with ambient light components. The response times of the LEDs and PDs were less than 10 μs, resulting in a sampling rate of approximately 10 kHz even with time-division control.

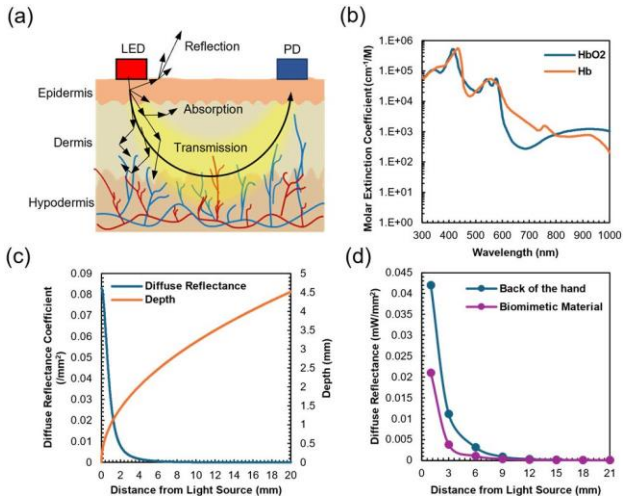

Fig. 6. Measurement principle of the flexible optical tactile force sensor. (a) Light scattering and reflection in skin. (b) Wavelength versus hemoglobin absorption. (c) Simulation of light scattering in tissue. (d) Measurements in simulants and back of the hand.

This measurement method satisfied the necessary performance requirements as the required sampling rate for tactile sensing is below 10 kHz [36].

B. Measurement Principle of the Flexible Optical Tactile Force Sensor

The proposed sensor configuration is similar to those of existing optical biosensors, such as PPG and SpO2 sensors. Based on the arrangement of the light-emitting and light-receiving components relative to the tissue, optical biosensors can be categorized into transmission and reflection types [37]. In transmission-type sensors, the light-emitting and light-receiving elements are positioned on opposite sides of the tissue, allowing the emitted light to traverse the skin and be received on the other side. Conversely, reflection-type sensors are designed with both elements positioned on the same side to detect light reflected from the skin. In both types, a portion of the light emitted from the light source is reflected at the tissue surface, whereas the remainder penetrates the tissue. Within the tissue, light undergoes multiple scatterings and some of this scattered light reaches the light-receiving element. The amount of light absorbed within the tissue changes with the blood volume and blood oxygen concentration at the measurement site, allowing for the acquisition of biological information, such as pulse rate and SpO2, from the detected light. The proposed sensor adopted a reflection-type configuration.

The skin comprises three main layers: epidermis, dermis, and subcutaneous tissue. When visible or infrared light irradiates the skin, it experiences scattering, absorption, and transmission within tissues [Fig. 6(a)]. Shorter wavelengths are more absorbed by hemoglobin in the blood, whereas longer wavelengths are more absorbed by water. Therefore, visible and near-infrared lights, which are less impacted by absorption by blood and water, are commonly employed in biosensing [Fig. 6(b)] [38]. PPG sensors often employ green light, which is highly absorbed by hemoglobin, to estimate arterial shape in devices, such as smartwatches. SpO2 sensors leverage the distinct absorption properties of near-infrared and red light for oxyhemoglobin and deoxyhemoglobin. Conversely, the proposed sensor prioritizes tissue penetration and exclusively utilizes longer wavelength near-infrared light. In this study, the 850-nm wavelength LED was selected owing to its lower absorption by hemoglobin and water compared with the 940-nm wavelength LED, resulting in higher optical transmittance and enhanced detection of changes within biological tissue.

When light irradiates the body, it penetrates deeper into the tissues through repeated absorption and scattering by the skin, blood, water, and other components. The depth of light penetration influences the effectiveness of absorption and multiple scattering. This penetration is not only impacted by the wavelength of the light but also by the distance between the light-emitting and receiving elements. The light propagation in a reflection-type optical sensor calculated using a multiple-scattering model that simulates biological tissue is shown in Fig. 6(c) [39]. The farther apart the light-emitting and receiving elements, the lesser the light received and the deeper the light that penetrates the tissue. Capillaries are typically located 0.1–0.2 mm below the skin surface, whereas arterioles are located at depths of 0.3–1 mm. Therefore, a distance of a minimum of 1 mm between the light-emitting and light-receiving elements is necessary. The experimental results of measuring light propagation with distances between 1 and 21 mm between the elements are shown in Fig. 6(d). The measurements affixed to the simulated biological materials demonstrated a strong positive correlation with the calculated values (correlation coefficient $r = 0.998$). Similarly, when the sensor was affixed to the back of the hand and measured under conditions of rest without applying pressure to the fingers, the correlation coefficient was $r = 0.988$, demonstrating an agreement between the experimental and calculated results.

The proposed sensor measured the amount of absorbed light that changed in response to the tissue deformation caused by the tactile force. This change was not only influenced by internal tissue deformation but also by alterations in skin shape and blood volume, all of which collectively impacted the amount of light absorption. For example, as the pressure on the fingertip increased, the finger's thickness decreased (Fig. 7), whereas its width increased. Because deformation altered the distance between the light-emitting and receiving elements, the shape of the tissue and interelement distance influenced the measurement. Additionally, pressure decreases the blood volume in the capillaries, resulting in changes in light absorption by the blood.

While previous studies focused on surface deformation or color changes of the skin, our proposed method incorporated internal tissue information, resulting in higher measurement accuracy. However, owing to individual variations in tissue deformation and the resulting changes in light absorption, calibration was required, as demonstrated in previous research [19].

C. Evaluation of Tactile Force Measurement Accuracy

The proposed sensor was affixed to the back of the hand for measurement to assess the accuracy of the tactile

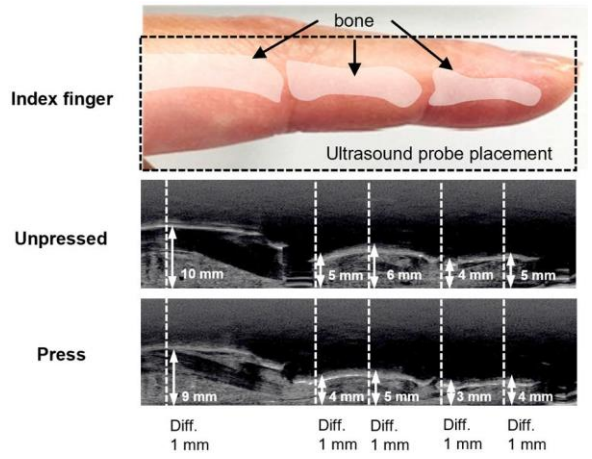

Fig. 7. Deformation of biological tissue in response to pressure on the finger. Internal structure of the index finger captured utilizing an ultrasound imaging device (SONIMAGE HS1, Konica Minolta).

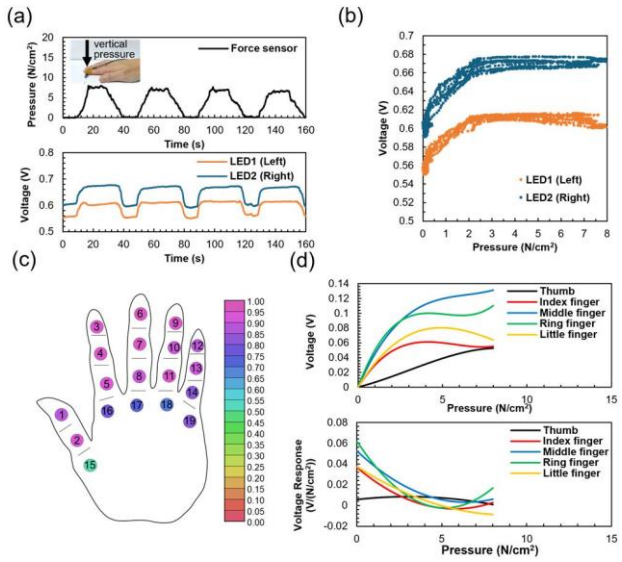

Fig. 8. Detection accuracy of the magnitude of tactile force. (a) Time-series data of outputs. (b) Output relation between sensors. (c) Correlation coefficient by site. (d) Fitting curves for distal phalanges.

force detection. The proposed and reference force sensors were utilized simultaneously. The proposed sensor was sequentially attached to different parts of the back of the right hand, whereas the reference sensor was pressed against the corresponding palm side at a contact angle of 0°. This setup allowed for the evaluation of the correlation between the signals measured using the proposed sensor and pressure values from the reference sensor.

The time-series measurement results when periodic pressure was applied to the distal phalanx of the index finger are shown in Fig. 8(a). The output of the proposed sensor was synchronized with the fluctuations in the output of the reference sensor. The process of pressing, maintaining pressure, and releasing were continuously performed at 5 s intervals. The voltage at each pressure point was determined through a single measurement. The correlation between the sensor outputs is shown in Fig. 8(b), with the average correlation coefficient r of the optical tactile force sensor measuring 0.81 in the pressure range of 0–8 N/cm^2. Furthermore, in the low-pressure range (0–3 N/cm^2), the average correlation coefficient r was 0.95, demonstrating a stronger positive correlation. Additionally, we observed a strong positive correlation with an average correlation coefficient (r) of 0.95 in the pressure range of 0–2 N/cm^2. However, in the 2–4 N/cm^2 range, the correlation coefficient decreased to 0.58. This decline in correlation could be attributed to the nonlinear response of the sensors to increasing pressure. Furthermore, in the 4–6 N/cm^2 range, r was −0.10, and in the 6–8 N/cm^2 range, r was 0.03. Beyond 4 N/cm^2, the signal intensity of the optical tactile force sensor reached saturation, resulting in a lack of correlation.

This saturation signifies the upper limit of tissue deformation and blood volume change in response to the tactile force at the measurement site, establishing the dynamic range of the proposed method for measuring the tactile force up to 3 N/cm^2. Additionally, the difference in the baseline voltage between LED2 and LED1 may be attributed to a misalignment in the sensor's attachment position.

To further demonstrate the feasibility of similar measurements on other parts of the hand and fingers, a reference force sensor utilizing MEMS was used to apply a maximum pressure of 8 N/cm^2 at the 19 locations, as shown in Fig. 8(c). The sensor was repositioned at each measurement point, and the correlation coefficient r was calculated. The results revealed an average r of 0.88, validating the ability to measure tactile force in areas other than the fingertips. The average values for the resolution, precision, and response times were 0.1 N/cm^2, 89%, and 0.5 s, respectively. The cubic polynomial approximation curves for each fingertip, indicating the variation in the signal intensity and its first derivative with the applied pressure at each measurement site are shown in Fig. 8(d). The diverse results of the first derivative suggest that skin deformation in response to tactile force differed across various locations.

These results demonstrate that by attaching the proposed sensor to the back of the hand, high-precision detection of tactile forces can be achieved without compromising tactile sensation throughout the entire hand. Because these measurements are not limited to specific areas, such as the fingertips, broader applications are anticipated. Notably, variations in skin properties and hand morphology among individuals may influence the measurement results. However, the proposed method enables stable measurements across various areas, necessitating further optimization to enhance consistency across different participants.

D. Evaluation of Estimation Accuracy in the Direction of Tactile Force

Identifying not only the magnitude but also the direction of the tactile force is essential for various applications in human interfaces. The direction of the tactile force directly influences the stability of objects, and humans interact with both the magnitude and direction of the tactile force when interacting with objects. Furthermore, the friction force at the contact surface is influenced by the direction of the tactile force [40], [41], [42], [43], [44].

As previously mentioned, the proposed sensor can measure both the magnitude and direction of the tactile force through

the time-division control of the light-emitting components. The sensor can distinguish between left–right and up–down pressure directions with high accuracy by utilizing specific LED drive combinations, as shown in Fig. 1(c). First, the sensor was attached to the distal phalanx of the index finger, and changes in the signal intensity of the optical tactile force sensor were measured when pressure was applied in the left–right direction, as shown in Fig. 9(a). The amount of light received from the left-side LED1 and right-side LED2 varied depending on the direction of the applied pressure. The direction of the applied pressure was estimated using clustering upon the removal of pulse signals and noise from the measurement data [Fig. 9(b)]. The sensor achieved an accuracy of 98% in distinguishing up–down directions [Fig. 9(c)] and 100% accuracy in distinguishing left–right directions [Fig. 9(d)].

Furthermore, this experiment was conducted at 14 distinct locations surrounding each joint of all fingers. The average identification accuracy was 99% in the left–right direction and 94% in the up–down direction [Fig. 9(e) and (f)]. The variance in accuracy is attributed to the anatomical structure of the fingers, where the skin experiences less deformation in the up–down direction compared with the left–right direction [45].

IV. Discussion

We developed a novel measurement technology that can be attached to the back of the hand and fingers, facilitating the detection of both the magnitude and direction of the tactile force without hindering tactile sensation. Furthermore, the sensor components were affixed to a flexible substrate, enabling measurements to be performed without causing discomfort or pressure even when worn on the fingers. These features render the technology highly suitable for sensing applications in human interfaces.

The evaluation results demonstrated an r of 0.95 between the proposed sensor output and tactile force within the range of up to 3 N/cm^2, signifying that tactile force can be estimated with high accuracy. Furthermore, the direction of the tactile force was estimated with an accuracy of over 94%. These findings underscore the superiority of the proposed method, which can evaluate areas beyond the fingertips that were previously challenging to measure. Although the accuracy in detecting the up–down direction was slightly lower than that for the left–right direction, enhancements could be made by increasing the number of light-emitting and receiving elements, as well as incorporating machine learning techniques.

In the proposed sensor system, the critical factors of wiring, power consumption, and spatial resolution were crucial for ensuring measurement reliability and practical implementation. These aspects should be considered as future research challenges. Regarding wiring, the current system employs a wired connection. However, for wearable applications, user comfort is paramount for practical deployment, necessitating the transition to wireless communication. In terms of power consumption, optimizing efficiency through wavelength selection of the light source and enhancing the sensitivity of the PD are promising approaches worth considering. Spatial resolution is a key parameter for obtaining detailed pressure distribution. Implementing a multiwavelength sensor array could enable higher precision measurements.

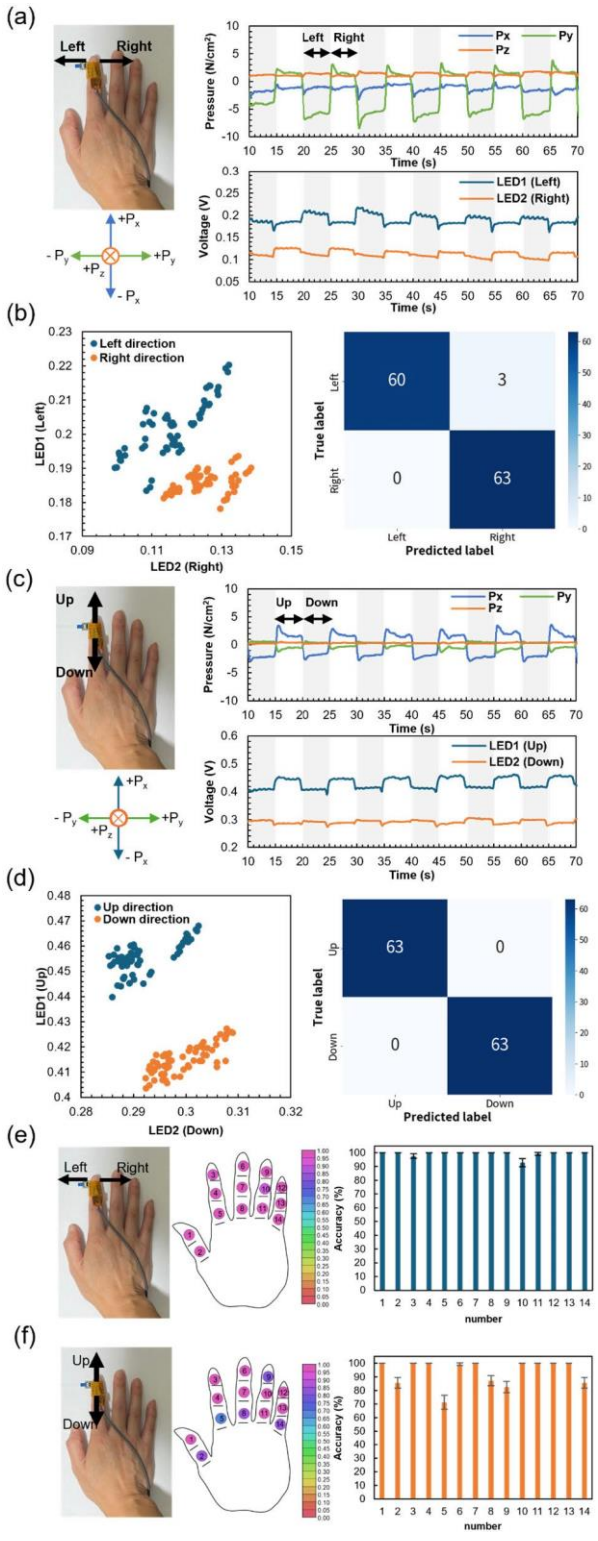

Fig. 9. Detection accuracy of the direction of the tactile force. (a) Measurement for left–right direction. (b) Voltage relationship and estimation for left–right LEDs. (c) Measurement for up–down direction. (d) Voltage relationship and estimation for up–down LEDs. (e) Accuracy for left–right direction. (f) Accuracy for up–down direction.

The quantitative evaluation of tactile sensation is crucial, with its applications being explored in numerous fields. In the medical field, this technology can aid in assessing

the functional recovery of patients' limbs and guiding effective rehabilitation. In robot-assisted surgery, it can provide surgeons with more precise tactile feedback while operating instruments. Additionally, in sports and cosmetics, it can enhance training efficiency and convey the expertise of skilled practitioners. The proposed method offered a solution that enabled tactile force sensing without compromising tactile sensation, paving the way for the practical implementation of various promising applications.

V. Conclusion

In this study, we developed a flexible optical tactile force sensor that can be attached to the back of the hand and fingers, allowing for the detection of both the magnitude and direction of tactile force without compromising tactile sensation. The proposed method enabled noninvasive and high-precision measurement of tactile information and offered physiological insights through the simultaneous acquisition of pulse wave data. Evaluation results demonstrated a high correlation coefficient within the tactile force range of up to 3 N/cm^2 and an accuracy of over 94% for direction detection. These findings indicate that the sensor can be applied to areas of the hand beyond the fingertips, which were previously challenging to measure. Although the accuracy in detecting the up–down direction was slightly lower than that for the left–right direction, further enhancements are anticipated by increasing the number of light-emitting and receiving elements and incorporating machine-learning techniques. Additionally, improvements in wiring, power consumption, and spatial resolution are required. The adoption of wireless communication is crucial for ensuring user comfort and optimizing battery efficiency. Furthermore, improving spatial resolution requires the implementation of a higher precision sensor array. Moreover, considering the influence of individual differences on measurements, the development of algorithms to address sensor misalignment and measurement site variations is imperative. This will lead to more accurate measurement results and the development of a device that can cater to a diverse range of users.

This technology is expected to enhance diagnostic capabilities through real-time monitoring of mechanical and cardiovascular data in the medical field while improving the accuracy of tactile force measurement and enabling comprehensive performance evaluation in sports. The proposed flexible optical tactile force sensor can significantly enhance the performance and reliability of tactile interfaces across various applications, including healthcare and sports.

References

[1] Y. Luo et al., "Adaptive tactile interaction transfer via digitally embroidered smart gloves," *Nature Commun.*, vol. 15, no. 1, p. 868, Jan. 2024.

[2] K. Kim, H. Yang, J. Lee, and W. G. Lee, "Metaverse wearables for immersive digital healthcare: A review," *Adv. Sci.*, vol. 10, no. 31, Nov. 2023, Art. no. 2303234.

[3] M. Zhu et al., "Haptic-feedback smart glove as a creative human-machine interface (HMI) for virtual/augmented reality applications," *Sci. Adv.*, vol. 6, no. 19, p. 8693, May 2020.

[4] R. Cobo, J. García-Piqueras, J. Cobo, and J. A. Vega, "The human cutaneous sensory corpuscles: An update," *J. Clin. Med.*, vol. 10, no. 2, p. 227, Jan. 2021.

[5] A. Zimmerman, L. Bai, and D. D. Ginty, "The gentle touch receptors of mammalian skin," *Science*, vol. 346, no. 6212, pp. 950–954, Nov. 2014.

[6] T. Sagisaka, Y. Ohmura, Y. Kuniyoshi, A. Nagakubo, and K. Ozaki, "High-density conformable tactile sensing glove," in *Proc. 11th IEEE-RAS Int. Conf. Humanoid Robots*, Bled, Slovenia, Oct. 2011, pp. 537–542.

[7] Z. Wang, J. Hoelldampf, and M. Buss, "Design and performance of a haptic data acquisition glove," in *Proc. 10th Annu. Int. Workshop Presence*, Jan. 2007, pp. 349–357.

[8] K. Matsuo, K. Murakami, T. Hasegawa, and R. Kurazume, "A decision method for the placement of tactile sensors for manipulation task recognition," in *Proc. IEEE Int. Conf. Robot. Autom.*, Pasadena, CA, USA, May 2008, pp. 1641–1646.

[9] J. Zhang et al., "Flexible wide-range multidimensional force sensors inspired by bones embedded in muscle," *Microsyst. Nanoeng.*, vol. 10, no. 1, p. 64, May 2024.

[10] R. Ono, S. Yoshimoto, and K. Sato, "Visual force sensing for deviceless interface with finger pushing onto palm," *J. Inst. Image Inf. Telev. Eng.*, vol. 68, no. 7, pp. J285–J291, 2014.

[11] M. Nakatani and T. Kawasoe, "Haptic skill logger (HapLog): The wearable sensor for evaluating haptic behaviors," *J. Robot. Soc. Jpn.*, vol. 30, no. 5, pp. 499–501, 2012.

[12] S. A. Mascaro and H. H. Asada, "Understanding of fingernail-bone interaction and fingertip hemodynamics for fingernail sensor design," in *Proc. 10th Symp. Haptic Interfaces Virtual Environ. Teleoperator Syst. HAPTICS*, Mar. 2002, pp. 106–113.

[13] K. Sakuma et al., "Wearable nail deformation sensing for behavioral and biomechanical monitoring and human–computer interaction," *Sci. Rep.*, vol. 8, no. 1, p. 18031, Dec. 2018.

[14] Y. Sun, J. M. Hollerbach, and S. A. Mascaro, "Estimation of fingertip force direction with computer vision," *IEEE Trans. Robot.*, vol. 25, no. 6, pp. 1356–1369, Dec. 2009.

[15] J. Chen et al., "Three-dimensional arterial pulse signal acquisition in time domain using flexible pressure-sensor dense arrays," *Micromachines*, vol. 12, no. 5, p. 569, May 2021.

[16] M. S. Sarwar et al., "Touch, press and stroke: A soft capacitive sensor skin," *Sci. Rep.*, vol. 13, no. 1, p. 17390, Oct. 2023.

[17] G. Vega et al., "VARitouch: Back of the finger device for adding variable compliance to rigid objects," in *Proc. CHI Conf. Hum. Factors Comput. Syst.*, New York, NY, USA, May 2024, pp. 1–20.

[18] H. Mameno, M. Imura, Y. Uranishi, S. Yoshimoto, and O. Oshiro, "Estimation of fingertip contact force direction based on change in nail color distribution," *Jpn. J. Med. Eng.*, vol. 52, pp. 155–156, Jan. 2014.

[19] A. Saito, W. Kuno, W. Kawai, N. Miyata, and Y. Sugiura, "Estimation of fingertip contact force by measuring skin deformation and posture with photo-reflective sensors," in *Proc. 10th Augmented Hum. Int. Conf.*, New York, NY, USA, Mar. 2019, pp. 1–6.

[20] A. B. Hertzman, "The blood supply of various skin areas as estimated by the photoelectric plethysmograph," *Amer. J. Physiol.-Legacy Content*, vol. 124, no. 2, pp. 328–340, 1938.

[21] Y. Khan et al., "A flexible organic reflectance oximeter array," *Proc. Nat. Acad. Sci. USA*, vol. 115, no. 47, pp. E11015–E11024, Nov. 2018.

[22] H. Lee et al., "Toward all-day wearable health monitoring: An ultralow-power, reflective organic pulse oximetry sensing patch," *Sci. Adv.*, vol. 4, no. 11, p. 9530, Nov. 2018.

[23] G. Simone et al., "High-accuracy photoplethysmography array using near-infrared organic photodiodes with ultralow dark current," *Adv. Opt. Mater.*, vol. 8, no. 10, May 2020, Art. no. 1901989.

[24] H. Jinno et al., "Self-powered ultraflexible photonic skin for continuous bio-signal detection via air-operation-stable polymer light-emitting diodes," *Nature Commun.*, vol. 12, no. 1, p. 2234, Apr. 2021.

[25] F. Elsamnah, A. Bilgaiyan, M. Affiq, C.-H. Shim, H. Ishidai, and R. Hattori, "Reflectance-based organic pulse meter sensor for wireless monitoring of photoplethysmogram signal," *Biosensors*, vol. 9, no. 3, p. 87, Jul. 2019.

[26] S. Park et al., "Ultraflexible near-infrared organic photodetectors for conformal photoplethysmogram sensors," *Adv. Mater.*, vol. 30, no. 34, Jul. 2018, Art. no. 1802359.

[27] J. Allen, "Photoplethysmography and its application in clinical physiological measurement," *Physiological Meas.*, vol. 28, no. 3, pp. R1–R39, Feb. 2007.

[28] M. Wang, Z. Li, Q. Zhang, and G. Wang, "Removal of motion artifacts in photoplethysmograph sensors during intensive exercise for accurate heart rate calculation based on frequency estimation and notch filtering," *Sensors*, vol. 19, no. 15, p. 3312, Jul. 2019.

[29] Y. Maeda, M. Sekine, T. Tamura, T. Suzuki, and K.-I. Kameyama, "Comparison of measurement sites and light sources in photoplethysmography during walking," *Jpn. J. Med. Eng.*, vol. 49, no. 1, pp. 132–138, Jan. 2011.

[30] Y. Zhang et al., "Motion artifact reduction for wrist-worn photoplethysmograph sensors based on different wavelengths," *Sensors*, vol. 19, no. 3, p. 673, Feb. 2019.

[31] Y. Lee et al., "Standalone real-time health monitoring patch based on a stretchable organic optoelectronic system," *Sci. Adv.*, vol. 7, no. 23, p. 9180, Jun. 2021.

[32] G. H. Lee et al., "Stretchable PPG sensor with light polarization for physical activity–permissible monitoring," *Sci. Adv.*, vol. 8, no. 15, p. 3622, Apr. 2022.

[33] J. Park, H. S. Seok, S.-S. Kim, and H. Shin, "Photoplethysmogram analysis and applications: An integrative review," *Frontiers Physiol.*, vol. 12, Mar. 2022, Art. no. 808451.

[34] S. Li, L. Liu, J. Wu, B. Tang, and D. Li, "Comparison and noise suppression of the transmitted and reflected photoplethysmography signals," *BioMed Res. Int.*, vol. 2018, pp. 1–9, Sep. 2018.

[35] H. Liu, Y. Wang, and L. Wang, "The effect of light conditions on photoplethysmographic image acquisition using a commercial camera," *IEEE J. Transl. Eng. Health Med.*, vol. 2, pp. 1–11, 2014.

[36] C. Connor, S. Hsiao, J. Phillips, and K. Johnson, "Tactile roughness: Neural codes that account for psychophysical magnitude estimates," *J. Neurosci.*, vol. 10, no. 12, pp. 3823–3836, Dec. 1990.

[37] T. Tamura, "Current progress of photoplethysmography and SPO_2 for health monitoring," *Biomed. Eng. Lett.*, vol. 9, no. 1, pp. 21–36, Feb. 2019.

[38] S. Prahl. *OMLC: Optical Absorption of Hemoglobin*. Accessed: Nov. 6, 2024. [Online]. Available: https://omlc.org/spectra/hemoglobin/

[39] M. S. Patterson, S. Andersson-Engels, B. C. Wilson, and E. K. Osei, "Absorption spectroscopy in tissue-simulating materials: A theoretical and experimental study of photon paths," *Appl. Opt.*, vol. 34, no. 1, pp. 22–30, Jan. 1995.

[40] R. S. Johansson and G. Westling, "Roles of glabrous skin receptors and sensorimotor memory in automatic control of precision grip when lifting rougher or more slippery objects," *Exp. Brain Res.*, vol. 56, no. 3, pp. 550–564, Oct. 1984.

[41] B. P. Delhaye, F. Schiltz, F. Crevecoeur, J.-L. Thonnard, and P. Lefèvre, "Fast grip force adaptation to friction relies on localized fingerpad strains," *Sci. Adv.*, vol. 10, no. 3, p. 9344, Jan. 2024.

[42] S. Ding, Y. Pan, M. Tong, and X. Zhao, "Tactile perception of roughness and hardness to discriminate materials by friction-induced vibration," *Sensors*, vol. 17, no. 12, p. 2748, Nov. 2017.

[43] S. Lee et al., "Nanomesh pressure sensor for monitoring finger manipulation without sensory interference," *Science*, vol. 370, no. 6519, pp. 966–970, Nov. 2020.

[44] B. P. Delhaye, E. Jarocka, A. Barrea, J.-L. Thonnard, B. Edin, and P. Lefèvre, "High-resolution imaging of skin deformation shows that afferents from human fingertips signal slip onset," *eLife*, vol. 10, p. 64679, Apr. 2021.

[45] M. Wiertlewski and V. Hayward, "Mechanical behavior of the fingertip in the range of frequencies and displacements relevant to touch," *J. Biomechanics*, vol. 45, no. 11, pp. 1869–1874, Jul. 2012.

Kosuke Ando received the B.Eng. degree in energy science and engineering and the M.Eng. degree in applied quantum physics and nuclear engineering from Kyushu University, Fukuoka, Japan, in 2013 and 2015, respectively. He is currently pursuing the Ph.D. degree in science, technology, and innovation with Kobe University, Kobe, Japan.

In 2015, he joined Konica Minolta, Tokyo, Japan, where he developed optical devices. His current research interests include biosensing technology.

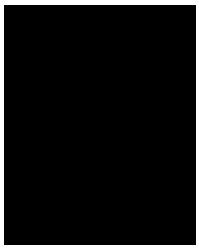

Minon Kushihashi (Graduate Student Member, IEEE) received the B.E. degree in computer and systems engineering from Kobe University, Kobe, Japan, in 2023, where she is currently pursuing the master's degree.

Her current research interests include the development of sensing devices to enhance cosmetic application techniques.

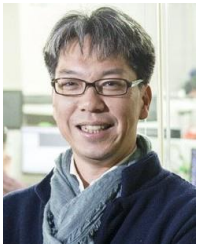

Hiroshi Kawaguchi (Member, IEEE) received the B.Eng. and M.Eng. degrees in electronic engineering from Chiba University, Chiba, Japan, in 1991 and 1993, respectively, and the Ph.D. degree in electronics engineering from The University of Tokyo, Tokyo, Japan, in 2006.

In 1993, he joined Konami Corporation, Kobe, Japan, where he developed arcade entertainment systems. He was a Technical Associate with the Institute of Industrial Science, The University of Tokyo, in 1996 and appointed as a Research Associate, in 2003. In 2005, he was a Research Associate with the Graduate School of Engineering, Kobe University, Kobe, Japan. From 2015 to 2016, he was a Visiting Researcher with Politecnico di Milano, Milan, Italy. Since 2016, he has been a Full Professor at the Graduate School of Science, Technology and Innovation, Kobe University. He is also a Collaborative Researcher with the Institute of Industrial Science, The University of Tokyo. His current research interests include low-voltage operating circuits, soft error characterization and mitigation, ubiquitous sensor networks, organic semiconductor circuits, data converters, healthcare devices, and neurocomputer architecture.

Dr. Kawaguchi is a member of ACM and IEICE. He was a recipient of IEEE ISSCC 2004 Takuo Sugano Outstanding Paper Award, the ACM/IEEE ASP-DAC 2013 University Design Contest Best Design Award, and the IEEE ICECS 2016 Best Paper Award. He has served as a Design and Implementation of Signal Processing Systems (DISPS) Technical Committee Member for the IEEE Signal Processing Society; a Technical Program Committee Member for the IEEE International Conference on Acoustics, Speech and Signal Processing (ICASSP), the IEEE Global Conference on Signal and Information Processing (GlobalSIP), the IEEE Workshop on Signal Processing Systems (SiPS), the IEEE Custom Integrated Circuits Conference (CICC), and the IEEE Symposium on Low-Power and High-Speed Chips (COOL Chips); and as an Organizing Committee Member for the IEEE Asian Solid-State Circuits Conference (A-SSCC); and the ACM/IEEE Asia and South Pacific Design Automation Conference (ASP-DAC). He was an Associate Editor of *Journal of Signal Processing Systems* (Springer), *IEICE Transactions on Fundamentals of Electronics, Communications and Computer Sciences, IEICE Transactions on Electronics*, and *IPSJ Transactions on System LSI Design Methodology* (TSLDM).

Shintaro Izumi (Member, IEEE) received the B.Eng. and M.Eng. degrees in computer science and systems engineering, and the Ph.D. degree in engineering from Kobe University, Kobe, Japan, in 2007, 2008, and 2011, respectively.

He was a JSPS Research Fellow at Kobe University, from 2009 to 2011, an Assistant Professor with the Organization of Advanced Science and Technology, Kobe University, from 2011 to 2018, and an Associate Professor with the Institute of Scientific and Industrial Research, Osaka University, Suita, Japan, from 2018 to 2019. Since 2019, he has been an Associate Professor with the Graduate School of System Informatics, Kobe University. His current research interests include biomedical signal processing, communication protocols, low-power very large scale integration (VLSI) design, and sensor networks.

Dr. Izumi served as a Technical Committee Member for the IEEE Biomedical and Life Science Circuits and Systems, a Student Activity Committee Member for the IEEE Kansai Section, and a Program Committee Member for the IEEE Symposium on Low-Power and High-Speed Chips (COOL Chips). He was a recipient of the 2010 IEEE SSCS Japan Chapter Young Researchers Award. He was the Chair of the IEEE Kansai Section Young Professionals Affinity Group.